Analysis of pedestrian dynamics in counter flow via an extended lattice gas model

Hua Kuang,[1,2,*] Xingli Li,[3] Tao Song,[1] and Shiqiang Dai[1,†]
[1]*Shanghai Institute of Applied Mathematics and Mechanics, Shanghai University, Shanghai, 200072, China*
[2]*College of Physics and Electronic Engineering, Guangxi Normal University, Guilin 541004, China*
[3]*School of Applied Science, Taiyuan University of Science and Technology, Taiyuan 030024, China*
(Received 8 April 2008; published 29 December 2008)

The modeling of human behavior is an important approach to reproduce realistic phenomena for pedestrian flow. In this paper, an extended lattice gas model is proposed to simulate pedestrian counter flow under the open boundary conditions by considering the human subconscious behavior and different maximum velocities. The simulation results show that the presented model can capture some essential features of pedestrian counter flows, such as lane formation, segregation effect, and phase separation at higher densities. In particular, an interesting feature that the faster walkers overtake the slower ones and then form a narrow-sparse walkway near the central partition line is discovered. The phase diagram comparison and analysis show that the subconscious behavior plays a key role in reducing the occurrence of jam cluster. The effects of the symmetrical and asymmetrical injection rate, different partition lines, and different combinations of maximum velocities on pedestrian flow are investigated. An important conclusion is that it is needless to separate faster and slower pedestrians in the same direction by a partition line. Furthermore, the increase of the number of faster walkers does not always benefit the counter flow in all situations. It depends on the magnitude and asymmetry of injection rate. And at larger maximum velocity, the obtained critical transition point corresponding to the maximum flow rate of the fundamental diagram is in good agreement with the empirical results.

DOI: 10.1103/PhysRevE.78.066117 PACS number(s): 89.40.−a, 45.70.Vn, 05.50.+q, 05.70.Fh

I. INTRODUCTION

In recent years, the modeling of pedestrian flows has become one of the most exciting topics and has attracted considerable attention in the field of physical science and engineering [1–4]. This increasing interest is stimulated not only by its practical application for optimizing pedestrian facilities and management, but also by the observed self-organization phenomena and collective behavior in panic situations such as "freezing by heating" [5], the "faster-is-slow" effect [6], and herding behavior [6].

The typical pedestrian flows have been simulated with various models, such as the social force model [7,8], the centrifugal force model [9], the hydrodynamic models [10,11], the mean field equation models [12], cellular automaton models [13–19], and lattice gas models [20–36]. Since the lattice gas models and the cellular automaton models are conceptually simpler and can be easily implemented on computers for numerical investigations, they have found wider applications in simulating the evacuation behaviors [20,21], counter channel flow [23–36], and bottleneck flow [22]. Especially, as a typical model in counter flow modeling, the lattice gas model has been studied for counter flow in different situations. Muramatsu *et al.* [23] found that the jamming transition occurs in the pedestrian counter flow within a channel when the density is higher than a threshold. Muramatsu and Nagatani [24] investigated the jamming transition in the counter flow composed of four-way pedestrians at a crossing and compared the results with those of two-way counter flow. Takimoto *et al.* [25] studied the effect of the partition line on the pedestrian counter flow. It was shown that the partition line has a significant effect on the counter flow and enhances the critical flow and density. Fukamachi and Nagatani [26] simulated the pedestrian counter flow sidling through the crowd. It was found that the sidle has an important effect on the jamming transition of pedestrian flow. Yu and Song [16,27] modeled the pedestrian counter flow in a channel with considering the surrounding environment and the traffic rule breaking behavior. The counter flows in different scenarios, such as those in a T-shape channel [28], with the effects of following the front pedestrians in the same direction [29], with exchanging positions between face-to-face pedestrians [30], with different velocities [31] and mixed drift coefficients [32,33], with different sizes of slender particles [34,35], and in places where people are going on all fours [36], have also been investigated.

It is well known that pedestrian flow is a complex system with multiagents [37]. The movements of pedestrians are usually very complex and distinct in nature. The different pedestrians may have different walking habits (e.g., some people like to walk faster than others and some people prefer to walk slowly due to sex, age, etc.). And the same types of pedestrians may have the same subconscious behaviors which is also called preferential walking habits (e.g., people prefer to walk on the right-hand side of road [19] and pedestrians with the same velocities follow each other in the same direction in order to walk comfortably, securely, etc). Therefore, the modeling of pedestrian flow should fully globally consider these different factors or the mutual connection to study special phenomena and reproduce pedestrian dynamics in a realistic way. However, in previous studies, the majority of the models were based on spatial partition of different scenarios rather than human walking habits, and the individualities of pedestrians and common characteristics among pedestrians have not been perfectly distinguished in counter

*khphy@shu.edu.cn
†Corresponding author; sqdai@shu.edu.cn

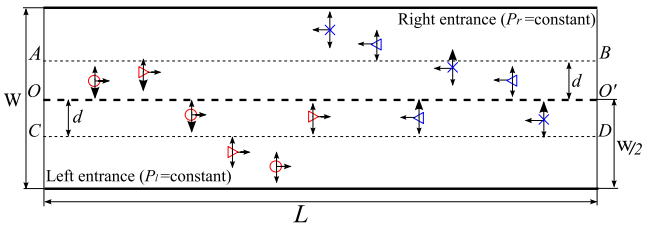

FIG. 1. (Color online) Sketch of the pedestrian counter flow. The top and bottom sides of the channel are walls. The faster (slower) walkers going to the right and to the left are indicated, respectively, by right triangles (circle) and left triangles (cross). Arrows indicate possible moving directions of the two groups. The bold arrow indicates the moving direction for walkers with subconscious behavior, i.e., different kinds of pedestrians would subconsciously cross different partition lines. For example, the faster (slower) right walker may walk towards the right-hand side and cross the central partition line OO' (or partition line CD) of the channel. And the faster (slower) left walkers have similar situations.

flow. This is not in agreement with the real situation, where different pedestrians might have different or similar subconscious behaviors and walking speeds. How do these factors affect the pedestrian dynamics in the counter flow? This is an interesting but still open problem. In this paper, the subconscious behavior will be mainly manifest in the following three aspects. First, walkers (including faster walkers and slower walkers) are accustomed to walking along a certain side of the road (e.g., the right-hand side in China; however, in some walkways and stairways, the left-hand side in Japan, and hereafter we only consider the scenarios in China) in order to avoid colliding with others in the opposite direction. Secondly, slower walkers prefer to move to the right-hand side of the road. It reflects the fact that slower walkers commonly consider themselves to be more comfortable and secure when moving near the right boundary of the road because they obey traffic rules and need not overtake others. Finally, faster walkers are used to overtaking the preceding walkers in the same direction from the left-hand side of the road.

In this paper, we establish an extended lattice gas model to investigate the pedestrian counter flow with different subconscious behaviors and different maximum velocities under the open boundary conditions. The pedestrian dynamics is discussed in greater detail. In the following section, the extended lattice model is presented for the pedestrian counter flow in a channel. Section III gives simulation results and discussion, followed by conclusions in the final section.

II. MODEL

The model is defined on a square lattice of $W \times L$ sites, where W and L are, respectively, the width and length of the channel, as shown in Fig. 1. There are four classes of pedestrians: faster or slower walkers going to the right and faster or slower walkers to the left. Each site contains only a single walker and each walker moves to the preferential direction with no back step. The walker is inhibited from overlapping at each site, and the excluded-volume effect is taken into account. When a walker arrives at the wall of channel, he/she will be reflected by the wall and never go out through the wall. The left and right boundaries are open. The injection rate P_l of the right walkers from the lower half of the left boundary is set to be a constant, and the injection rate of the faster (slower) right walkers is $P_l P_{fr}[P_l P_{sr} = P_l(1-P_{fr})]$. The injection rate P_r of the left walkers from the upper half of the right boundary is set to be another constant, and the injection rate of the faster (slower) left walkers is $P_r P_{fl}[P_r P_{sl} = P_r(1-P_{fl})]$. The right (left) walker goes into the channel from the lower (upper) half of the left (right) boundary, proceeds through the channel and goes out of the right (left) boundary. When the right (left) walker arrives at the right (left) boundary, he/she is removed from the channel.

We extend the lattice gas model of pedestrian flow [23,25] to take into account different maximum velocities and subconscious behavior of walkers in a channel. Figure 1 shows the pedestrian counter flow within a channel. The top and bottom of the channel are walls. The faster (slower) walkers going towards the right and the left are indicated, respectively, by right triangles (circle) and left triangles (cross). Arrows indicate the possible moving directions of the four groups. The bold arrow indicates the moving direction of walkers with subconscious behavior, i.e., different kinds of pedestrians would subconsciously cross different partition lines, e.g., the faster (or slower) right walkers may walk towards their right-hand side and cross the central partition line OO' (or partition line CD) of the channel. In this study, we assume that the walkers have the tendency to walk to the right-hand side. In other words, this subconscious behavior means the convention of sideways direction preference during their movement in a crowd. The parameter d represents the distance between the partition line CD and the central partition line OO', which reflects the fact that the influence region of subconscious behavior of faster walkers and slower walkers are different, i.e., when the faster (slower) right walkers are situated in the lower region of the partition line $OO'(CD)$, their subconscious behaviors will disappear due to arriving at the comfortable and secure walking region which they take for granted. Similarly, the faster (slower) left walkers have the same situations.

Figure 2 gives all the possible configurations of the faster and slower walkers going to the right. The full circle indicates the right walker. The cross point indicates the site occupied by the other walkers or the wall. Each walker can move only to the unoccupied sites. The transition probabilities $p_{t,x}$, $p_{t,y}$, and $p_{t,-y}$ of the right walker corresponding to each configuration are given by the following:

$p_{t,x}=D_1+(1-D_1)/3$, $p_{t,y}=(1-D_2)(1-D_1)/3$, and $p_{t,-y}=(1+D_2)(1-D_1)/3$ for configuration (a); $p_{t,x}=D_1+(1+D_2)(1-D_1)/2$, $p_{t,y}=(1-D_2)(1-D_1)/2$, and $p_{t,-y}=0$ for configuration (b); $p_{t,x}=D_1+(1-D_2)(1-D_1)/2$, $p_{t,y}=0$, and $p_{t,-y}=(1+D_2)(1-D_1)/2$ for configuration (c); $p_{t,x}=0$, $p_{t,y}=(1-D_2)/2$, and $p_{t,-y}=(1+D_2)/2$ for configuration (d); $p_{t,x}=1$, $p_{t,y}=0$, and $p_{t,-y}=0$ for configuration (e); $p_{t,x}=0$, $p_{t,y}=1$, and $p_{t,-y}=0$ for configuration (f); $p_{t,x}=0$, $p_{t,y}=0$, and $p_{t,-y}=1$ for configuration (g); $p_{t,x}=0$, $p_{t,y}=0$, and $p_{t,-y}=0$ for configuration (h), where D_1 indicates the strength of the drift pointing to the exits (right or left), and D_2 represents the strength of the preferential direction of subconscious behavior. As D_2

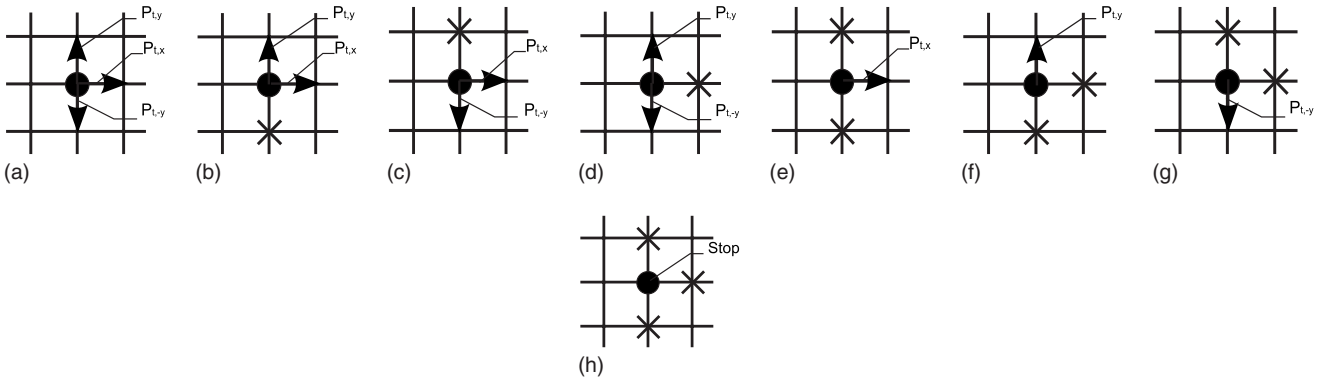

FIG. 2. All the possible configurations of the faster and slower walkers going to the right on a square lattice. The full circle indicates the right walker. The cross point indicates the site occupied by another walker or the wall. The walker can move only to the unoccupied sites. The transition probabilities to the nearest-neighbor sites (to the right, up, and down) are given by $P_{t,x}$, $P_{t,y}$, and $P_{t,-y}$, respectively.

$=0$, the subconscious behavior is not considered and our model reduces to the original model presented in Ref. [24]. For convenience, we call the case of $D_2=0$ unsubconscious behavior, otherwise, the case of $D_2 \neq 0$ subconscious one.

Different kinds of walkers have different subconscious behaviors under different circumstances. We implement the pedestrians' subconscious behaviors by varying the values of D_2 from the following three aspects.

(1) When the walkers are situated in the upper region of the partition lines (central partition line OO' for the faster walkers and partition line CD for the slower walkers), they have the priority to move on the right-hand side of the walkway, and in this case, $D_2 \neq 0$, otherwise, $D_2=0$.

(2) When the walkers are situated in the lower region of the partition lines (central partition line OO' for the faster walkers and partition line CD for the slower walkers), the faster walkers would be accustomed to overtaking the preceding slower walkers in the same direction from the left-hand side, and in such a case, $D_2 \neq 0$ and the transition probability $P_{t,y}$ is replaced with $P_{t,-y}$ for the configuration (d), otherwise (e.g., when the preceding walkers are faster right walkers, the walkers have no subconsciousness of the overtaking; this reflects the fact that the same type of walkers follow each other and form human trail formation, which is interpreted by Helbing as self-organization effect due to nonlinear interactions among persons [7]), $D_2=0$.

(3) When the walkers encounter the opposite walkers, wherever they are situated in the road, they always walk from the right-hand side so as to avoid collisions for the configuration (d), and in this case, $D_2 \neq 0$, otherwise, $D_2=0$.

For a left walker, similar prescriptions can be given for the possible configurations. In this study, we introduce a movement rule similar to the FI cellular automaton model of vehicular flow (see Ref. [38]) for simulating pedestrian movement with different maximum velocities. The walkers will move forward for $x(n)$ cells in one update time step if the transition probability $p_{t,x}$ is met, where $x(n) = \min[V_{\max}(n), \mathrm{gap}(n)]$, $V_{\max}$ denotes the maximum velocity of the nth walker, and $\mathrm{gap}(n)$ denotes the number of empty cells in front of the nth walker. Because pedestrians are mostly intelligent and flexible, they can accelerate to maximum velocity in a short time, and correspondingly this movement rule can describe the real pedestrian flow well.

III. SIMULATION RESULTS AND DISCUSSIONS

Using the model and the open boundary conditions described above, we carried out the simulation for pedestrian counter flow. In the unit time step, all walkers within the channel are updated only once. The update procedure is the random sequential rule. Initially, there are no walkers within the channel. The right (left) walkers are distributed randomly on the left (right) boundary with the injection rate $P_l(P_r)$. All the walkers are numbered randomly from 1 to N, where N is the total number of walkers existing within the channel, including the walkers on the boundaries. Following the rule in Fig. 2, the numbered walkers are in order updated. After all the walkers have been updated, if the walkers in the channel arrive at the boundaries, they are removed from the channel. In the next time step, new right and left walkers are added on

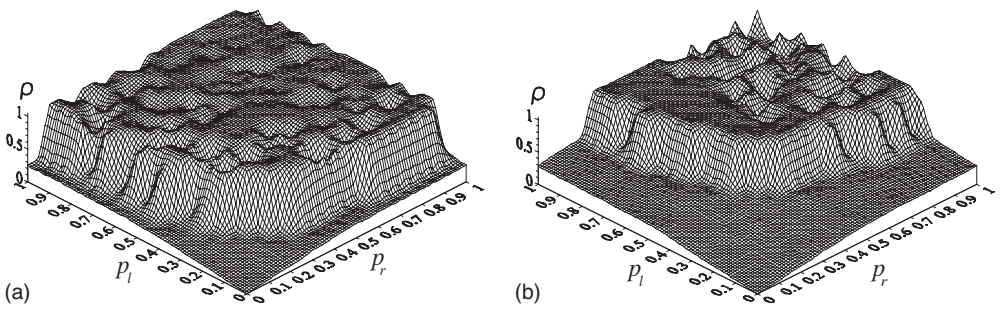

FIG. 3. Comparisons of 3D plots between (a) the unsubconscious behavior and (b) subconscious behavior.

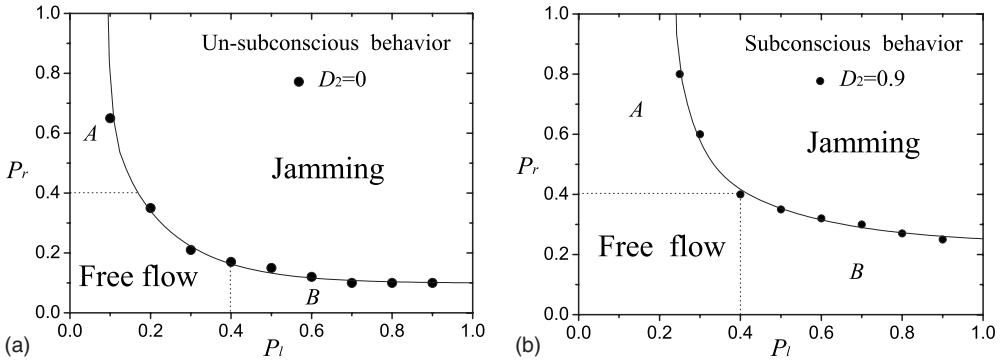

FIG. 4. Comparison of phase diagrams corresponding to the 3D plots in Fig. 3 between (a) the case without subconscious behavior and (b) the case with subconscious behavior, where the solid line is the fitting curve, i.e., the critical density curve.

the left and right boundaries as the walker densities on both boundaries remain to be P_l and P_r. Then the above procedure is repeated.

For simplicity, only the case of $V_{\max,fr}=V_{\max,fl}=V_{\max,1}$ and $V_{\max,sr}=V_{\max,sl}=V_{\max,2}$ is considered in this paper, where $V_{\max,fr}$, $V_{\max,sr}$, $V_{\max,fl}$, and $V_{\max,sl}$ are the maximum velocities for the faster right walker, the slower right walker, the faster left walker, and the slower left walker, respectively. In the simulations, the related parameters are taken as $W=20$, $L=100$, $d=5$, $V_{\max,1}=3$ and $V_{\max,2}=1$, $P_{fr}=P_{fl}=0.5$, $D_1=0.6$ and $D_2=0.9$ unless otherwise mentioned.

The mean velocity $\langle V\rangle$ in one update time step is defined as the sum of the velocities of walkers moving forward divided by the total number of walkers existing in the channel. The mean occupancy ρ of pedestrian is defined as the total number of walkers in the channel divided by the channel area $(W\times L)$. For each simulation, 10 000 time steps are run, and the value of $\langle V\rangle$ and ρ are computed according to the last 4000 time steps averaged over 20 runs.

The 3D plot of the mean occupancy ρ against the injection rate P_l and P_r with the unsubconscious behavior ($D_2=0$) and subconscious behavior ($D_2=0.9$) are shown in Figs. 3(a) and 3(b), respectively. From Fig. 3, it can be clearly seen that the phase transition from freely moving phase to completely jamming phase happens. Compared with Fig. 3(a), Fig. 3(b) corresponds to a larger (smaller) region of the freely moving (the jamming) state. In other words, subconscious behavior, to some extent, could retard the occurrence of the jam. We have also found some density fluctuations at higher injection rate, which correspond to the different completely jammed cases. In some regions, the density is high but does not attain 1, which means the walkers in the channel are segregated one or more region than one completely jammed region [see Fig. 6(c)]. However, in other regions, where the density is equal to 1, the segregation regions do not appear and the channel will be fully occupied by pedestrians [see Fig. 6(f)]. The results show that all kinds of complicated interactions caused by the subconscious effect and random distribution lead to diverse completely jammed states.

In order to gain a deeper insight into the phase transition, we plot the phase diagram with unsubconscious behavior ($D_2=0$) and subconscious behavior ($D_2=0.9$) in Figs. 4(a) and 4(b) corresponding to that of 3D plot in Figs. 3(a) and 3(b), respectively. The freely moving and the jamming regions are divided by a solid line, i.e., the critical density curve. Obviously, the freely moving region in Fig. 4(a) is smaller and the jamming region is larger compared with those in Fig. 4(b). We have also found that the freely moving regions A and B are almost not completely symmetric for $P_l>0.4$ and $P_r>0.4$ because of the existence of statistical error and the influence of random distribution during the calculating and simulating. However, at the border between the freely moving phase and the jamming phase, there is a hint of a metastable state. This state will be discussed later in detail (see Fig. 8). Actually, the sizes of the different regions

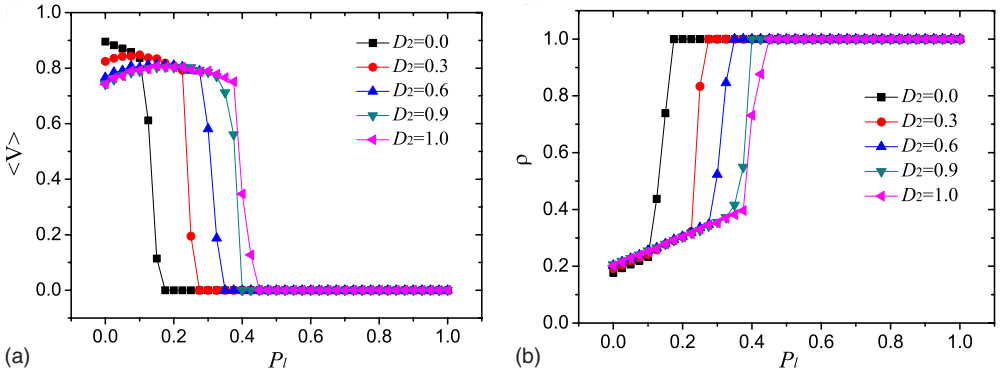

FIG. 5. (Color online) Plot of the mean velocity $\langle V\rangle$ (a) and the mean occupancy ρ (b) against the injection rate P_l with the changing parameter $D_2=0,0.3,0.6,0.9,1$, where $P_r=0.4$, $P_{fr}=P_{fl}=0.5$, $D_1=0.6$.

depend considerably on D_2 and the increase of D_2 will lead to the expansion (shrinkage) of the freely moving (jamming) region. From these observations we can conclude that the subconscious behavior has an important influence on the pedestrian flow. It could effectively decrease the occurrence of jam cluster.

We will now focus on analyzing the influence of the subconscious behavior. The best way is to investigate the effect of the strength of D_2 on pedestrian dynamics. Figure 5 gives (a) the plot of the mean velocity $\langle V \rangle$ and (b) the mean occupancy ρ against the injection rate P_l with the changing parameter $D_2=0,0.3,0.6,0.9,1$, where $P_r=0.4$, $P_{fr}=P_{fl}=0.5$, $D_1=0.6$. From this figure, it can be clearly seen that with the increase of D_2, the critical value of P_l increase, i.e., the jamming transition point moves to the right and jams do not occur easily. In addition, we also find that in the freely moving phase, on the contrary, the increase of D_2 leads to the decrease of $\langle V \rangle$. This is because at the low injection rate, the occupancy of channel is low, and in such a case, the pedestrians without the subconscious behavior could move randomly so as to avoid collision, which enhances the road utilization and decreases the interaction of pedestrian. But with increasing P_l, the available road area is reduced. At this time, if the pedestrians still move unconsciously, the interaction among pedestrians will be rapidly strengthened, and consequently the jams appear. However, if the walkers move subconsciously, the faster and slower walkers may be separated in the same directions and the interaction of them will be weakened, therefore, the jams will obviously decrease. All these reflect the walkers' subconscious behavior and has a passive effect at lower density and a positive effect at higher density for counter flow in the freely moving state.

Next we investigate the flow patterns at the free moving phase and observe the jamming transition evolution. Figure 6 shows the typical patterns obtained. The pattern (a) shows the freely moving phase at $P_r=P_l=P_{fr}=P_{fl}=0.3$ and (b) at $P_r=P_l=0.3$ and $P_{fr}=P_{fl}=0.8$. It shows that there is not appreciable difference between Figs. 6(a) and 6(b) at the same injection rate except that the number of pedestrians in Fig. 6(b) is less than that in Fig. 6(a). This is because the faster walkers could move out of the channel quickly, which causes the decrease in the occupancy, and thereby, enhances the capacity of channel. However, we can clearly see that the patterns in Figs. 6(a) and 6(b), where walkers intend to move along the right-hand side of the channel with the same maximum velocity, which is consistent with the empirically confirmed development of dynamically varying lanes [17]. In addition, in the region near the central partition line, we can also find an interesting feature for the counter flow that the faster walkers overtake the slower walkers from the left-hand side and then form a narrow-sparse walkway. This segregation effect of lane formation is the result of the walkers' subconscious behavior and interactions. Walkers moving in a mixed crowd or moving against the stream will lead to frequent and strong interactions. In each interaction, the encountering pedestrians move a little aside due to subconscious behavior in order to pass each other. In such a case, on the one hand, walkers have the tendency to move along the right-hand side, which causes the separation of the oppositely moving walkers. On the other hand, they have the tendency to overtake the preceding walkers from the left-hand side, which makes different walkers with the different maximum velocities in the same direction separate. Moreover, once the pedestrians move in uniform lanes, the interaction among them will be weakened. The simulation results further validate that in freely moving phase, there are always four lanes of walkers with different walking directions and velocities.

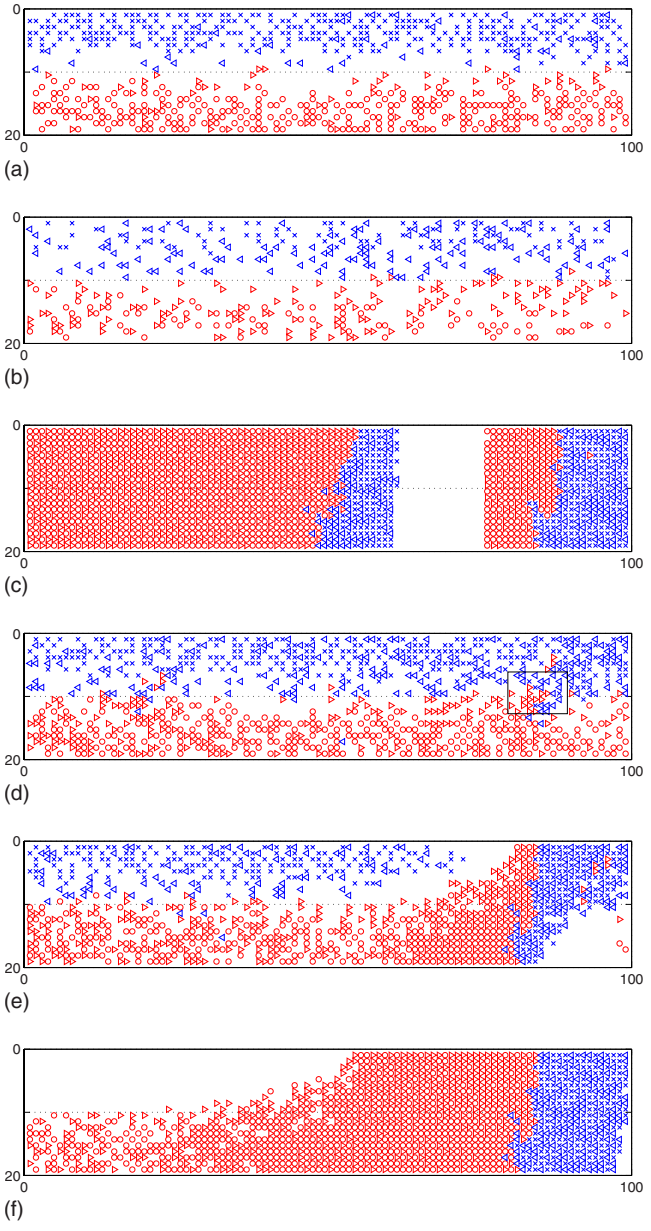

FIG. 6. (Color online) The typical patterns obtained where $L=100$, $W=20$, $D_1=0.6$, and $D_2=0.9$. The pattern (a) and (b) show the freely moving phase obtained at $P_r=P_l=P_{fr}=P_{fl}=0.3$, $P_r=P_l=0.3$, and $P_{fr}=P_{fl}=0.8$, respectively. The pattern (c) shows the completely jammed phase obtained at $P_r=0.4$, $P_l=0.6$, and $P_{fr}=P_{fl}=0.5$. The patterns (d)–(f) show the time evolution of the completely jamming transition for $P_r=P_l=P_{fr}=P_{fl}=0.5$, (d) the pattern obtained at $t=500$, (e) the pattern obtained at $t=580$, and (f) the pattern obtained at $t=900$.

The pattern (c) shows the completely jammed phase obtained at P_r=0.6, P_l=0.4, and P_{fr}=P_{fl}=0.5. The patterns (d)–(f) show the time evolution of the jamming transition for P_r=P_l=P_{fr}=P_{fl}=0.5 at t=500,580,900, respectively. In the beginning, most of pedestrians can move freely. At the same time, small jam clusters form occasionally [see Fig. 6(d)], and with the time evolution, these cluster jam clusters grow [see Fig. 6(e)]. These emerged clusters show that jamming is mainly caused by oppositely moving faster walkers [see rectangle in Fig. 6(d)] and getting jammed with each other. Since there is no back step movement, once the oppositely moving walkers get jammed they can only move sideways and occasionally forwards. While the already jammed pedestrians try to move out of existing jam clusters, the other moving pedestrians get jammed with the existing clusters making these clusters grow larger and larger with time, and finally will cause a complete blockage [see Fig. 6(f)]. At the jamming phase, the jam cluster does not move and is stationary within the channel. In such a case, the walkers' subconscious behavior and different maximum velocities have no effect on the jam cluster in the completely jamming state.

How do faster walkers affect the crowd counter flow? To elucidate this point, we plot the mean velocity $\langle V\rangle$ and the occupancy ρ against P_{fr} for various values of P_r and P_l in Fig. 7. Here we discuss the effects of the symmetrical and asymmetrical injection rate on the crowd flow in detail for the following four cases, respectively.

First, as P_r and P_l are small and symmetrical (e.g., P_r =P_l=0.1,0.2,0.3), the increase of P_{fr} could be helpful for the improvement of road utilization. This is because in such a case, there are not many walkers in the channel and nearly all the walkers can move forward freely, therefore, the increase in the number of faster walkers could lead to the gradual increase of the mean velocity $\langle V\rangle$ and, correspondingly, the gradual decrease of the mean occupancy ρ. Secondly, as P_r and P_l are both large, regardless of symmetry or asymmetry (e.g., P_r=P_l=0.4 and P_r=0.4, P_l=0.5), the mean velocity $\langle V\rangle$ becomes zero and ρ goes to 1.0, namely, the completely jammed phase occurs and P_{fr} has no influence on the pedestrian counter flow. Thirdly, it should be noted that for this case with a larger asymmetrical injection rate such as P_r=0.1, P_l=0.8, the counter flow is separated to two independent opposite unidirectional pedestrian flows, where the pedestrians can move freely and the completely jammed stage never occurs.

Lastly, when P_r and P_l are moderately asymmetrical, e.g., P_r=0.6 and P_l=0.3, another interesting phenomenon that P_{fr} has a significant negative influence on the pedestrian counter flow can be found. From Fig. 7, we can see that the average velocity $\langle V\rangle$ decreases and the mean occupancy ρ increases gradually with the increase of P_{fr}. This is because when the system attains its stability, the number of total pedestrians becomes larger and the value of occupancy is greater than 0.7, which indicates the interaction of walkers becomes stronger. And then the further increase of faster walkers could lead to the increase of those walkers overtaking from the left, especially near the central partition line, where the left and right faster walkers would invade the walkway where the opposite walkers move, namely, they move beyond their respective walking routes. As a result, with the strengthening of their interaction, minijams originally occur near the partition line, then extend to the road sides and finally form the completely megajams. This can also be clearly seen in Figs. 6(d)–6(f). From the four cases, we can find that the necessary condition for the appearance of jamming phase is that the occupancy must be large enough to cause the fast walkers to overtake from not their own routes but others', so the value of occupancy is at least 0.5. Based on the above analysis, the mechanism of jamming phase can be thoroughly explored. This surprising result shows that the jamming phase is mainly caused by the overtaking of faster walkers. In other words, the increase of the number of faster walkers is not always positive to the counter flow in all situations. It depends on the magnitude and asymmetry of the injection rate.

Figure 8 exhibits the time evolution of (a) the mean velocity $V(t)$ and (b) the occupancy $\rho(t)$ for different values of P_r and P_l under the symmetrical and asymmetrical conditions. Here we only give the first 5000 time steps. For the small and rather large injection rates, the velocity and occupancy reach quickly the steady values, that is to say, in such a case, the system has only a steady state, i.e., either the freely moving state for P_r=P_l=0.2 or completely jammed state for P_r=P_l=0.6. However, it should be noted that for the larger injection rate P_r=P_l=0.4 under the symmetrical condition and P_r=0.6, P_l=0.3 under the asymmetrical condition, there are two steady states: one is a metastable state and the other is completely jammed state. With the time evolution, the number of pedestrian increases and the mean velocity

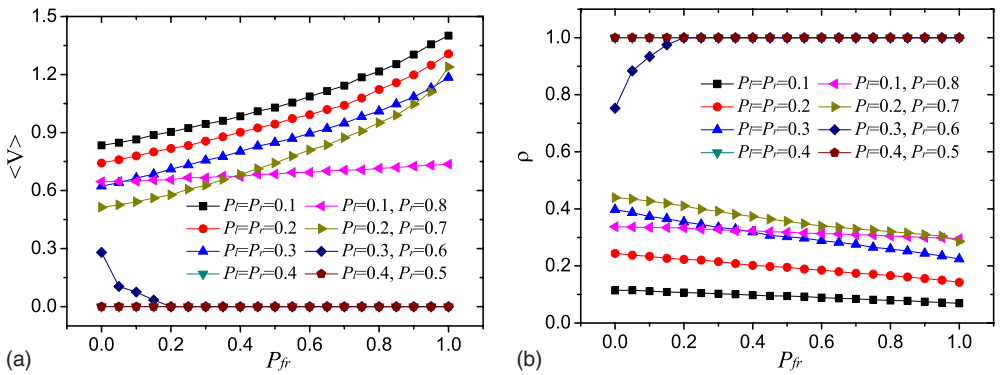

FIG. 7. (Color online) Plot of the mean velocity $\langle V\rangle$ (a) and the mean occupancy ρ (b) against the faster pedestrian fraction P_{fr} for different combinations of P_r and P_l, where D_1=0.6, D_2=0.9, and P_{fl}=0.5.

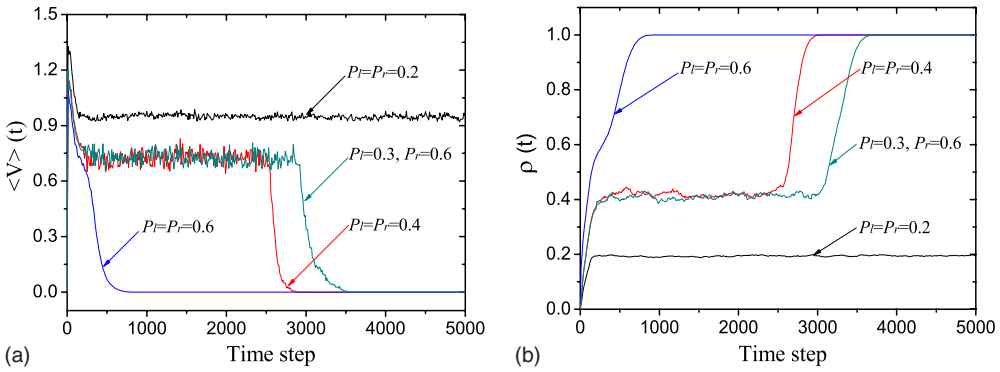

FIG. 8. (Color online) Time evolution of (a) the velocity $V(t)$ and (b) the occupancy $\rho(t)$ for the system size $L=100$, $W=20$ at the injection rate $P_r=P_l=0.2$, $P_r=P_l=0.4$, $P_r=P_l=0.6$, $P_r=0.6$, and $P_l=0.3$.

(density) decreases (increases) to a stable value. At this time, the system is in the metastable state, in which the interaction among pedestrian strengthens, forming small jam clusters. However, the system can break up the small clusters when the jammed pedestrians in these clusters succeed in moving past each other, thereby dissolving the clusters. This process can keep a long time. But with the further increase of time, pedestrians may get jammed with the existing clusters, which make these clusters grow further and thus the larger jam clusters come into being. Eventually the system can run into a jam with this mechanism, at the same time, the mean velocity (density) decreases (increases) to 0(1), which means the system transits to the completely jammed phase from the metastable state. However, for the case of $P_r=0.6$, $P_l=0.3$, the evolution time in the metastable state is longer than that of the case of $P_l=P_r=0.4$, which means that the small clusters would dissolve more easily under the asymmetrical condition.

What would happen if the parameter d has different values (i.e., the partition lines CD were located at different positions in the channel)? Should we draw partition lines in the channel to separate the different kinds of pedestrian similar to traffic flow on roads, where there are different fast or slow lanes? This is a problem of significance. We introduce a dimensionless coefficient $R_d=d/(W/2)$ to denote the fraction of the channel width. Figure 9 shows the plot of the mean velocity $\langle V\rangle$ and the mean occupancy ρ against R_d for different P_r and P_l combinations in the freely moving phase. It can be clearly observed that R_d has little influence on the pedestrian dynamics at the lower density (e.g., $P_l=P_r=0.1$), while it has a slight influence at the higher density (e.g., $P_l=P_r=0.3$), where the mean velocity $\langle V\rangle$ gradually increases first and then decreases with the increase of the R_d. This is because pedestrians are more flexible than vehicles, and can adjust their behavior according to the different surrounding circumstances, e.g., the faster walkers can move forward not only on their own lanes but also on the lane of slower walkers in the same direction when there are no slower walkers in front of them. Based on an overall consideration of various factors, we may reach the conclusion that it is needless to separate faster and slower pedestrians in the same direction by a partition line in the channel.

Finally we study the behavior of different maximum velocities mixed pedestrian flow. Figure 10 shows the mean velocity $\langle V\rangle$ and the occupancy ρ against P_l for various values of $V_{\max,1}$ and $V_{\max,2}$. We assume that V_{sum} is the sum of $V_{\max,1}$ and $V_{\max,2}$, namely, $V_{\text{sum}}=V_{\max,1}+V_{\max,2}$. It can be clearly seen that the mean velocity $\langle V\rangle$ increases and the occupancy ρ decreases with the increase of V_{sum}. At the same time, the jamming transition occupancy also increases. At larger V_{sum}, the critical transition point corresponding to the maximum flow rate in the fundamental diagram is in good agreement with empirical results [31]. Here it should be noted that at the same values for V_{sum} (e.g., $V_{\max,1}=2$, $V_{\max,2}=2$ and $V_{\max,1}=3$, $V_{\max,2}=1$), the mean velocity $\langle V\rangle$ and the jamming transition point of symmetric condition

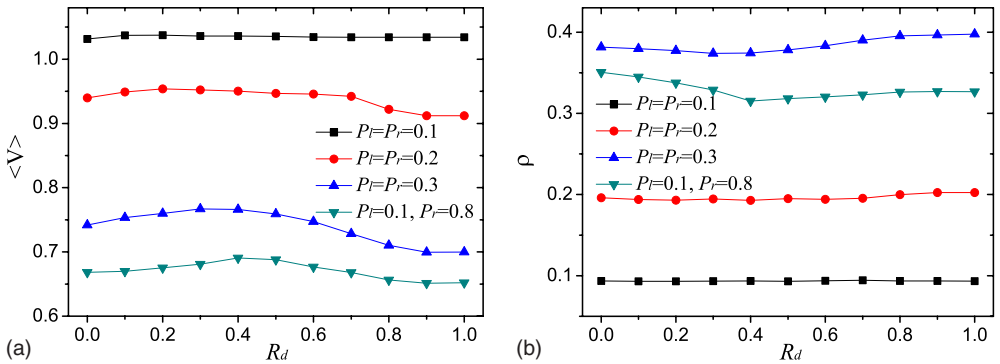

FIG. 9. (Color online) Plot of the mean velocity $\langle V\rangle$ (a) and the mean occupancy ρ (b) against dimensionless coefficient R_d for different combinations of P_r and P_l in the freely moving phase.

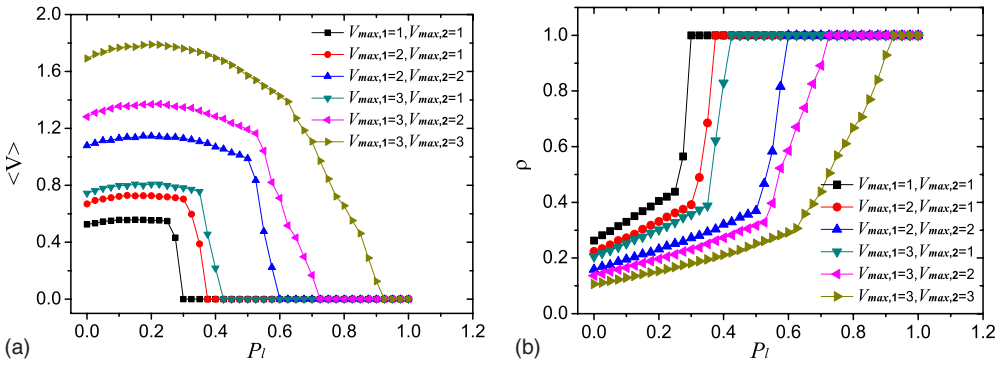

FIG. 10. (Color online) Plot of the mean velocity $\langle V \rangle$ (a) and the mean occupancy ρ (b) against the injection rate P_l with different maximum velocities $V_{\max,1}$ and $V_{\max,2}$ combinations, where $D_1=0.6$, $D_2=0.9$, $P_{fr}=P_{fl}=0.5$, and $P_r=0.4$.

$V_{\max,1}=V_{\max,2}$ are greater than those with asymmetric condition $V_{\max,1} \neq V_{\max,2}$, and correspondingly, the occupancy ρ with symmetric condition is lower than that with asymmetric condition. This is because when the maximum velocities are different, the slower walkers apparently interfere with the movement of the faster walkers. As a result, this makes the mean velocity $\langle V \rangle$ decline.

IV. CONCLUSIONS

The lattice gas model for pedestrian flow has attracted the interest of researchers in recent years. It has been applied to study the pedestrian flow in channels, the evacuation process, and the interaction between pedestrians and vehicles. However, it is unclear how the complex human preferential walking behaviors affect the pedestrian dynamics, especially when the maximum velocity of pedestrians is different. Up to now, these complex factors have not been completely taken into account for the lattice gas model in greater detail.

In this paper, an extended lattice gas model is proposed to investigate pedestrian counter flow under the open boundary conditions by considering the human subconscious behavior and the different maximum velocities, which can lead to appropriate responses to some complicated situations. The simulation results show that the presented model can capture some essential features of pedestrian counter flows, such as lane formation, segregation effect, and phase separation at higher densities. An especially interesting feature for counter flow is that the faster walkers overtake the slower ones and then form a narrow-sparse walkway, which can be observed in the region near the central partition line. Through the phase diagram analysis, we find that the subconscious behavior plays a key role in pedestrian dynamics, where the freely moving region is larger and the jamming region is smaller compared with the case of unsubconscious behavior. It could effectively decrease the occurrence of the jam cluster. Four cases about the influences of combinations of the symmetrical and asymmetrical injection rate are investigated. Comparison between them indicates different combinations could lead to different pedestrian phenomena. At larger injection rates, with time evolution, the system exhibits the metastable state and the completely jammed state under both symmetrical and asymmetrical conditions. Two important conclusions are reached. One is that it is needless to separate faster and slower pedestrian in the same direction by a partition line in the channel. The other is that the jamming phase is mainly caused by the overtaking of faster walkers. In other words, the increase of the number of faster walkers is not always positive to the counter flow in all situations. It depends on the magnitude and asymmetry of injection rate. Finally, we further investigate the influence of different combinations of maximum velocities $V_{\max}$ for slower and faster walkers on the pedestrian flow. And at large V_{sum}, the critical transition point corresponding to the maximum flow rate of the fundamental diagram is consistent with empirical results well.

ACKNOWLEDGMENTS

The authors would like to thank Professor Y. Xue, Dr. L.Y. Dong, Dr. J.P. Meng, and Ms. Y.F. Wei for helpful discussions and suggestions. This work was supported by the National Basic Research Program of China (Grant No. 2006CB705500), the National Natural Science Foundation of China (Grant Nos. 10532060, 10562001, and 10662002), the Shanghai Leading Academic Discipline Project (Grant No. Y0103) and Shanghai University Graduate Innovation Funds (Grant No. SHUCX080161).

[1] *Pedestrian and Evacuation Dynamics*, edited by M. Schreckenberg and S. D. Sharma (Springer-Verlag, Berlin, 2002).
[2] *Traffic and Granular Flow'03*, edited by S. P. Hoogendoorn, S. Luding, P. H. L. Bovy, M. Schreckenberg, and D. E. Wolf (Springer-Verlag, Berlin, 2005).
[3] D. Helbing, Rev. Mod. Phys. **73**, 1067 (2001).
[4] T. Nagatani, Rep. Prog. Phys. **65**, 1331 (2002).
[5] D. Helbing, I. J. Farkas, and T. Vicsek, Phys. Rev. Lett. **84**, 1240 (2000).
[6] D. Helbing, I. J. Farkas, and T. Vicsek, Nature (London) **407**,

487 (2000).
[7] D. Helbing and P. Molnar, Phys. Rev. E **51**, 4282 (1995).
[8] D. Helbing, L. Buzna, A. Johansson, and T. Werner, Transp. Sci. **39**, 1 (2005).
[9] W. J. Yu, R. Chen, L. Y. Dong, and S. Q. Dai, Phys. Rev. E **72**, 026112 (2005).
[10] R. L. Hughes, Transp. Res., Part B: Methodol. **36**, 507 (2002).
[11] R. L. Hughes, Annu. Rev. Fluid Mech. **35**, 169 (2003).
[12] T. Nagatani, Physica A **300**, 558 (2001).
[13] C. Burstedde, K. Klauck, A. Schadschneider, and J. Zittartz, Physica A **295**, 507 (2001).
[14] A. Kirchner, K. Nishinari, and A. Schadschneider, Phys. Rev. E **67**, 056122 (2003).
[15] V. J. Blue and J. L. Adler, Transp. Res., Part B: Methodol. **35**, 293 (2001).
[16] Y. F. Yu and W. G. Song, Phys. Rev. E **75**, 046112 (2007).
[17] W. G. Weng, T. Chen, H. Y. Yuan, and W. C. Fan, Phys. Rev. E **74**, 036102 (2006).
[18] A. Kirchner, H. Kluepfel, K. Nishinari, A. Schadschneider, and M. Schreckenberg, J. Stat. Mech.: Theory Exp. (2004) P10011.
[19] Y. Lizhong, L. Jian, and L. Shaobo, Physica A **387**, 3281 (2008).
[20] D. Helbing, M. Isobe, T. Nagatani, and K. Takimoto, Phys. Rev. E **67**, 067101 (2003).
[21] T. Nagatani and R. Nagai, Physica A **341**, 638 (2004).
[22] Y. Tajima, K. Takimoto, and T. Nagatani, Physica A **294**, 257 (2001).
[23] M. Muramatsu, T. Irie, and T. Nagatani, Physica A **267**, 487 (1999).
[24] M. Muramatsu and T. Nagatani, Physica A **286**, 377 (2000).
[25] K. Takimoto, Y. Tajima, and T. Nagatani, Physica A **308**, 460 (2002).
[26] M. Fukamachi and T. Nagatani, Physica A **377**, 269 (2007).
[27] Y. F. Yu and W. G. Song, Phys. Rev. E **76**, 026102 (2007).
[28] Y. Tajima and T. Nagatani, Physica A **303**, 239 (2002).
[29] M. Isobe, T. Adachi, and T. Nagatani, Physica A **336**, 638 (2004).
[30] L. Jian, Y. Lizhong, and Z. Daoliang, Physica A **354**, 619 (2005).
[31] R. Jiang and Q. S. Wu, Physica A **373**, 683 (2007).
[32] M. Fukamachi, R. Kuwajima, Y. Imanishi, and T. Nagatani, Physica A **383**, 425 (2007).
[33] Y. Imanishi, R. Kuwajima, and T. Nagatani, Physica A **387**, 2337 (2008).
[34] R. Nagai and T. Nagatani, Physica A **366**, 503 (2006).
[35] S. Ito, T. Nagatani, and T. Saegusa, Physica A **373**, 672 (2007).
[36] R. Nagai, M. Fukamachi, and T. Nagatani, Physica A **358**, 516 (2005).
[37] V. Grimm *et al.*, Science **310**, 987 (2005).
[38] Y. Ishibashi and M. Fukui, J. Phys. Soc. Jpn. **63**, 2882 (1994).